

A POLYMER DRIVESHAFT FOR USE IN
ORBITAL AND ROTATIONAL ATHERECTOMY

A thesis submitted to the faculty of
University of Minnesota
by

Preston Lee Grothe

in partial fulfillment of the requirements
for the degree of

Master of Materials Science and Engineering

Professor Russell J. Holmes

January 2016

Copyright © 2016 Preston Lee Grothe

All Rights Reserved

TABLE OF CONTENTS

List of Tables.....ii

List of Figures.....iii

Chapters

1.0 Introduction..... 1

2.0 Design of Polymer Driveshaft 3

3.0 Specifications and Acceptance Criteria 7

4.0 Products Tested 8

5.0 Test Method 9

6.0 Results 17

7.0 Conclusions.....28

8.0 Bibliography29

LIST OF TABLES

Table 1	List of available materials at the supplier and material properties	7
Table 2	Driveshaft requirements	7
Table 3	Tested Driveshaft Designs	8
Table 4	Driveshaft Testing Performed for Characterization.....	9
Table 5	Calculated bend stiffness values for the tested driveshafts, sorted in descending order. The currently used driveshafts are shaded.	18
Table 6	Buckle force and percent compression to kink for the tested driveshafts. The currently used driveshafts are shaded.....	19
Table 7	Calculated elastic torque response and maximum torque values for the tested driveshaft designs. The currently used driveshafts are shaded.	21
Table 8	Calculated slope from the elastic region, maximum load reached, and elongation to initial failure. The currently used driveshafts are shaded.....	23
Table 9	Ranking of driveshaft performance for each test. The current driveshafts (shaded) were used as the standard performance to be achieved. + 1 = Similar or better, 0 = Acceptable difference, -1 = Not close	25
Table 10	Results of the bend fatigue bend testing.	26

LIST OF FIGURES

Figure 1	Overview of the orbital atherectomy device.....	1
Figure 2	An illustration of a polymer driveshaft depicting the design features to address: 1. Accumulated Particulate, 2. Driveshaft Elongation, 3. Saline Flow Reduction, and 4. Required Lubrication.....	3
Figure 3	Axial view of a current driveshaft depicting the outer diameter, inner diameter, and wall thickness. A three-wire configuration of the current driveshaft is shown.....	4
Figure 4	Cross sectional view of tube depicting inner and outer radius dimensions.....	5
Figure 5	Image of the bend test setup	10
Figure 6	Driveshaft specimen placed into V-block.....	11
Figure 7	Pin gage or mandrel held down by magnetic V-block and holding driveshaft specimen in place	11
Figure 8	Diagram depicting gap between center beam and driveshaft and distance between edge of V-block and center beam.....	12
Figure 9	Left – An example of a block used to capture the bottom of the driveshaft. Right – The block is gripped in the pneumatic grips and holding the driveshaft.....	13
Figure 10	Left – Torque cell readout. Right – Torque test setup with pin vise grips. The vise grip on the left is connected to the torque cell and readout.....	14
Figure 11	Driveshaft gripped in pneumatic grips.	15
Figure 12	Driveshaft and guide wire tracked through the tight iliac model.	16
Figure 13	Load vs. Deflection curve for 5mm beam length stiffness test	17
Figure 14	Compression load vs. displacement curve for three of the driveshaft designs.	19
Figure 15	Torque vs. Rotation curve for one of the driveshaft designs	21
Figure 16	Load vs. Elongation curve for three driveshaft designs.....	23
Figure 17	Cross section of failed 8. Round coil, thick driveshaft	26
Figure 18	Cross section of failed 9. Round coil, med driveshaft	26
Figure 19	Cross section of an untested 8. Round coil, thick driveshaft. Note the wavy inner polyimide layer.....	27
Figure 20	Observed abrasion on the polyimide outer layer after life testing	27

1.0 INTRODUCTION

1.1 Background

This project was done as part of a technology research project at Cardiovascular Systems, Inc. Cardiovascular Systems, Inc. (CSI) is a manufacturer of medical devices that are used to treat peripheral and coronary artery disease. CSI's Orbital Atherectomy Devices (OADs) treat calcified and fibrotic plaque in arterial vessels throughout the leg and heart. The orbital atherectomy device contains an eccentrically mounted abrasive tool (crown) on a driveshaft. An electric control handle is used to drive rotation of the driveshaft. The driveshaft rotates up to 140,000 RPM over a guide wire and the eccentric crown generates centrifugal force, or orbital motion, in the confines of the vessel wall or lesion lumen. The crown has a diamond coated abrasive surface to sand away plaque material. The removed lesion material is released as particulate that is smaller than red blood cells and is reabsorbed by the blood stream. The orbital motion allows the crown to continue to sand away material and increase the lumen size with increased time in contact. A saline sheath is routed along the outer diameter of the driveshaft down to the crown location to provide lubrication and flushing at the treatment site. Figure 1 shows an overview of the orbital atherectomy device.

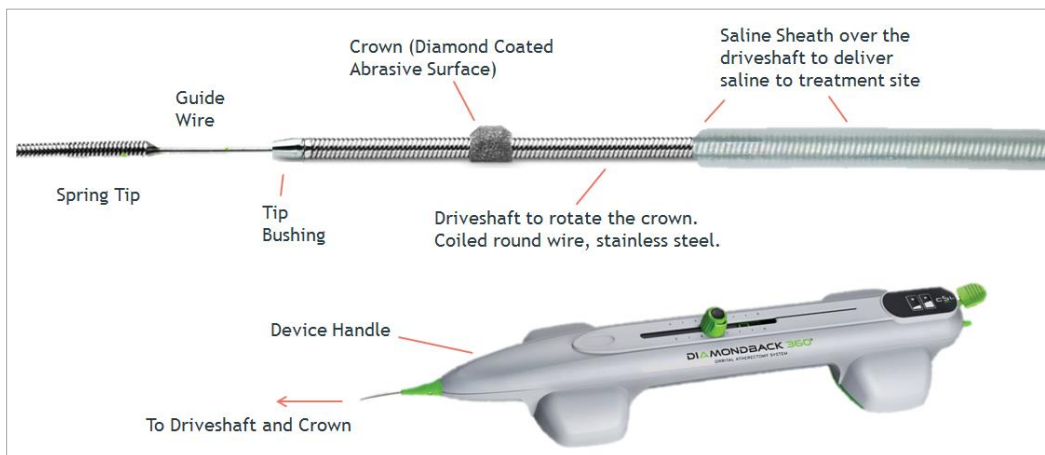


Figure 1 Overview of the orbital atherectomy device. [1]

The driveshaft, on which the crown is mounted, is comprised of coiled 304 stainless steel wires and the coils are formed with groups of three wires or more. The crown base

material is either 304 stainless steel or tungsten alloy. An abrasive coating, consisting of 30 micron size diamond particles, is adhered to the crown base material with a nickel alloy. The exposed diamond particles in the nickel alloy provide the sanding treatment while the crown rotates and orbits. The crowns can be either solder bonded or laser welded to the driveshaft.

1.2 Problem Statement

The current driveshaft allows the device to access and treat tortuous locations due to its flexible coiled wire design. At the same time, the driveshaft can treat tight diffuse locations without deforming or stalling due to its material strength. Although the current driveshaft design can provide successful treatment to challenging disease states, there is interest in an alternative driveshaft design to improve several characteristics that are inherent to the current driveshaft design.

1.2.1 Accumulated Particulate

The coiled driveshaft wires can flex and open during operation, which can allow particulate to penetrate into the driveshaft inner diameter. Particulate accumulation between the driveshaft and guide wire can cause binding and eventual seizure of the driveshaft.

1.2.2 Driveshaft Elongation

The driveshaft is constructed like a helical spring and can compress when it is delivered into the blood vessel. Stored compression in the driveshaft can result in driveshaft elongation and crown jumping upon device startup.

1.2.3 Saline Flow Reduction

The coiled driveshaft acts as an auger during rotation. The driveshaft is operated in a spin-to-open direction, which augers the fluid away from the treatment site and reduces the amount of saline flow during operation.

1.2.4 Required Lubrication

The driveshaft and the guide wire are comprised of 304 stainless steel and require the use of a lubricant during operation. Operating the driveshaft over the guide wire without lubrication can result in galling and eventual seizure of the driveshaft

due to the nickel content in the 304 stainless steel.

1.3 Project Objective

An alternative driveshaft design was investigated in this project. The new driveshaft was designed to improve upon the four characteristics listed above. The design approach was a polymer driveshaft construction, which is a metal coil or braid that contains polymer layers on the inside and outside diameters. The project objective was to determine if a polymer driveshaft design can perform to the same requirements as the current driveshaft design. Figure 2 shows an example polymer driveshaft with a coiled round wire configuration.

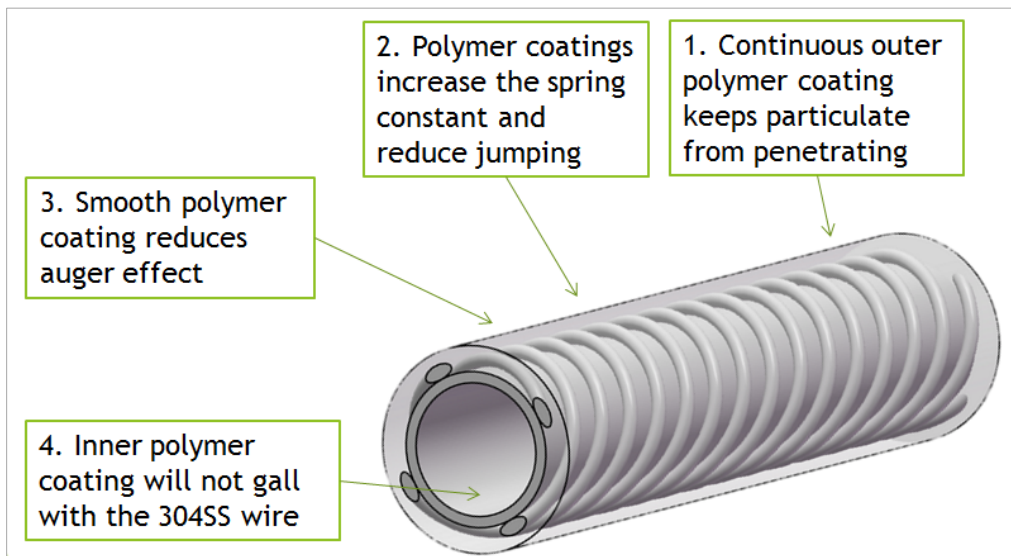


Figure 2 An illustration of a polymer driveshaft depicting the design features to address: 1. Accumulated Particulate, 2. Driveshaft Elongation, 3. Saline Flow Reduction, and 4. Required Lubrication

2.0 DESIGN OF POLYMER DRIVESHAFT

2.1 Supplier Capability

A current supplier of medical device components for CSI was used for constructing the polymer driveshafts tested in this project. The supplier has manufacturing capabilities to build polymer driveshaft constructions by single layers at a time and with tolerances of less than .001". The process is a reel to reel mandrel that passes through a polymer dip

coat process. This process coats the mandrel in very thin layers and the thickness is built up with additional passes through the dip coating. To build the polymer driveshaft, the mandrel is sized to the desired driveshaft inner diameter. It is then passed through the dip coating process to build the inner polymer layer to the chosen thickness. The mandrel is then passed through a braider or coiler to add the next layer of metal braid or coil right on top of the inner polymer layer. Finally, the reel is brought back to the polymer dip coating process and the outer layer is built up to the chosen thickness. Based on these capabilities, the polymer driveshaft designs evaluated in this project were comprised of a polymer inner layer, a middle layer metal coil or braid, and a polymer outer layer. The tested materials and configurations are listed below in section 4.

2.2 Dimensional Constraints

The new driveshaft dimensions must be similar to the current driveshafts. Figure 3 shows the range of dimensions for the current driveshafts.

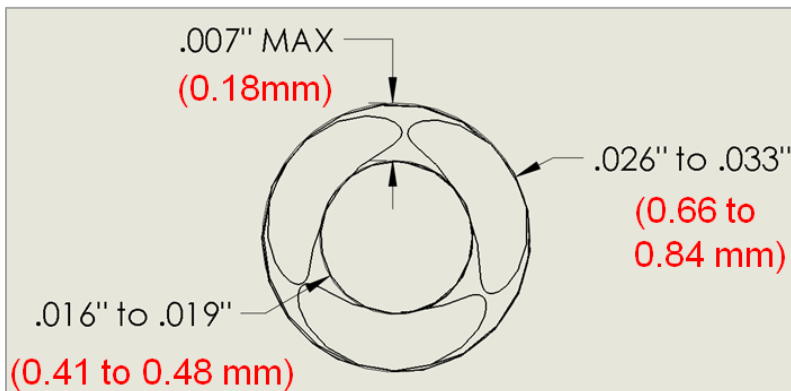


Figure 3 Axial view of a current driveshaft depicting the outer diameter, inner diameter, and wall thickness. A three-wire configuration of the current driveshaft is shown.

2.3 Driveshaft Materials Selection

The polymer driveshaft supplier materials currently used in medical devices include:

- Polyimide
- PolyTetraFluoroEthylene (PTFE)
- PTFE/Polyimide Composite (Proprietary Blend at Supplier)
- Nylon 12

- Polyether Block Amide (PEBAX)
- Polyurethane
- 304 stainless steel round and flat wire for coiling or braiding

For simplicity in initial material selection, the polymer driveshaft was considered to be a tube of solid polymer. Two of the main properties needed in a driveshaft are flexibility and push-ability. Flexibility can be measured by bend stiffness and push-ability can be measured by column strength. A current CSI driveshaft (see “current shaft 2” in section 4.0) was tested and used as baseline data for desired driveshaft performance. The elastic bend stiffness, or amount of force required to deflect the driveshaft in cantilever was approximately 0.7 lbf. per inch for a 5mm beam. See section 5.0 below for the test method on bend stiffness. This data point was used to back calculate the desired properties in a polymer for a solid polymer tube. The equation for relating elastic deflection and applied force is given in Equation 1 below;

$$\delta_{\max} = \frac{PL^3}{3EI} \quad [2] \quad (1)$$

Where δ_{\max} is maximum deflection, P is applied load, L is the beam length, E is Young’s Modulus, and I is the area moment of inertia. The area moment of inertia for a tubular structure is given in Equation 2 below;

$$I = \frac{\pi}{2} (r_o^4 - r_i^4) \quad [2] \quad (2)$$

Where r_o is the outer radius and r_i is the inner radius of the tube. These radius dimensions are depicted below in Figure 4.

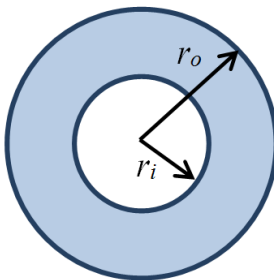


Figure 4 Cross sectional view of tube depicting inner and outer radius dimensions.

If, for example, a polymer tube has an outer diameter of .026” and wall thickness of

.003", this would give radius dimensions of $r_i = .010$ " and $r_o = .013$ ". This results in an area moment of inertia of $2.916 \cdot 10^{-8} \text{ in}^4$. With a beam length (L) of 5mm, a load versus deflection (P/δ_{max}) of 0.7 lbf/in., and an area moment of inertia of $2.916 \cdot 10^{-8} \text{ in}^4$, Equation 1 can be solved for Young's Modulus. This results in a Young's Modulus of 61,047 pounds per square inch (psi) or 0.42 Gigapascals.

The same exercise was done with column strength to back calculate the desired properties in a polymer for a solid polymer tube. The equation for column strength, or the buckle load of a column, is given in Equation 3 below;

$$F_{\text{buckle}} = \frac{\pi^2 EI}{(KL)^2} \quad [2] \quad (3)$$

Where K is a column effective length factor and is determined by the constraints on the top and bottom ends of the tested column. A column with one end fixed and one end free to rotate but not translate has a K factor of 0.699.

The current CSI driveshaft (see "current shaft 2" in section 4.0) was tested again and used as baseline data for desired driveshaft performance. See section 5.0 below for the test method on column strength. The column strength, or amount of axial compression force required to buckle the driveshaft, was approximately 0.08 lbf. for a 1 inch gage length.

With a column length (L) of 1 inch, a buckle force (F_{buckle}) of 0.08 lbf., a K factor of 0.699, and an area moment of inertia of $2.916 \cdot 10^{-8} \text{ in}^4$, Equation 3 can be solved for Young's Modulus. This results in a Young's Modulus of 135,838 pounds per square inch (psi) or 0.94 Gigapascals.

Table 1 shows a list of available polymer materials at the supplier. Polyimide and Nylon 12 (TR55LX) were chosen for testing based on their Young's Modulus values. The middle layers used in the polymer driveshafts were either coiled round wire, coiled flat wire, or braided flat wire. Since a polymer coating was added to both the outer and inner diameter and the wall thickness has a requirement of .007" maximum, the thickness of the coil or braid layer ranged from .0005 to .002 inches (12.7 to 50.8 microns).

Table 1 List of available materials at the supplier and material properties

Material	Elastic Tensile Modulus (psi)	Yield Strength (psi)	Moisture Absorption Immersed 23°C	Glass Transition Temp.	Hardness Shore D	Coeff. of Friction
Polyimide Type 100 HN ^[3]	370,000 (2.55 GPa)	10,000	2.8%	360 – 410°C	87	0.5
Nylon 12 TR55LX ^[3]	276,000 (1.90 GPa)	10,200	2.5%	110°C	82	0.45
PTFE ^[3]	50,000 to 90,000 flexural	1,350 – 4,350	<0.01%	115°C	50 - 65	0.1
PEBAX 55 ^[3]	22,600	1,740	1.2%	45°C	55	0.2 – 0.6
Polyurethane Tecoflex SG-60D ^[3]	13,000 flexural	*	*	*	51	*
304 Stainless For Comparison ^[4]	28,000,000	45,000	N/A	1400°C Solidus	Hardness is not measured in shore D scale	N/A

* Data unavailable

3.0 SPECIFICATIONS AND ACCEPTANCE CRITERIA

The design requirements for CSI driveshafts are shown in Table 2. The requirements were used to determine applicable properties and tests for characterizing polymer driveshafts.

Table 2 Driveshaft requirements

Driveshaft Requirement	Driveshaft Requirement	Applicable Properties / Tests
1	1. OAD must survive a life test after 2 high speed stalls 2. At high speed, the device shall have a maximum and a minimum dynamic stall torque value similar to current driveshafts	Torsional Rigidity Abrasion Resistance in Life Test (9 minute simulated operation)
2	OAD must exhibit track and push ability performance comparable to current OAD without kinking.	Column Strength Kink Resistance Bend Stiffness
3	Device must be easily removable from the introducer sheath with no damage to the device.	Tensile Strength
4	The device shall be designed for cyclic use: a total device life of 10.25 minutes spinning on high speed (140krpm) (6 sanding intervals plus 5 rest intervals)	Life Test (9 minute simulated operation) Bend Fatigue Test

Driveshaft Requirement	Driveshaft Requirement	Applicable Properties / Tests
5	Device driveshaft and connection to drive shaft hypotube shall be designed to withstand appropriate axial tensile load (applied incrementally) after completion of 9 minutes of high speed operation (life test).	Tensile Strength
6	All materials and manufacturing processes that are used for construction will not cause biological harm to the patient	Materials Selection (materials selected for testing are already commonly used in medical devices)

4.0 PRODUCTS TESTED

The driveshaft designs that were tested are shown below in Table 3. The polymer driveshaft samples were provided by the supplier and were selected based on similar dimensions to CSI driveshafts, and also to cover a variety of construction styles. Outer layer materials of Nylon 12 and Polyimide were selected for investigation based on the selection process in section 2.3. WPI means “wraps per inch” and PIC means “per inch crosses”. The quantities and build details are described in the procedure/method section.

Table 3 Tested Driveshaft Designs

Driveshaft	Outer Layer	Inner Layer	Middle Layer	ID (in.)	OD (in.)
1. Current Shaft 1 *	N/A	N/A	.006 304V Hyten round, 6 coil	0.019	0.031
2. Current Shaft 2 *	N/A	N/A	.0061 304V Hyten round, 3 coil	0.0163	0.0285
3. Braid, thick	PI	PI	.0005X.0025, 100 PIC, Braid	0.016	0.0256
4. Braid, thick 2	PI	PTFE	.0005X.0025, 110PIC, Braid	0.0168	0.0263
5. Flat coil, thick, Nylon	Nylon 12	PTFE	.0005X.003, 100WPI, Coil	0.0243	0.0319
6. Braid, thin	PI	PTFE	.0005X.0025, 100PIC, Braid	0.0165	0.0216
7. Flat coil, thin	PI	PI	.0005X.003, 175WPI, Coil	0.0176	0.0226
8. Round coil, thick	PI	PI	.002 round, 120 WPI, Coil	0.0182	0.0283
9. Round coil, med	PI	PI	.002 round, 120 WPI, Coil	0.0182	0.0258

10. Round coil, thick, Nylon	Nylon 12	PI	.002 round, 120 WPI, Coil	0.0184	0.0282
11. Round coil, med 2	PI	PI	.002 round, 127WPI, Coil	0.0154	0.0223
12. Flat coil, thin	Nylon 12	PTFE	.0005X.003, 100WPI, Coil	0.0243	0.029
13. Round coil, thin	PI	PI	.0015 round, 175WPI, Coil	0.0167	0.022
14. Flat coil, thin 2	PI	PTFE	.0005X.003, 100WPI, Coil	0.0247	0.0277
15. Flat coil, thin 3	PI	PTFE	.0005X.0025, 125WPI, Coil	0.0168	0.02
16. Flat coil, thin 4	PI	PI	.0005X.0025, 110WPI, Coil	0.0149	0.0182
17. Braid, med	PI	PI	.0005X.0025, 110PIC, Braid	0.0165	0.022

*Current metal coiled driveshaft designs

5.0 TEST METHOD

Testing was performed to characterize several driveshaft properties. The properties were selected based on required performance of the driveshaft. The properties and tests selected for the initial feasibility are listed below in Table 4.

Table 4 Driveshaft Testing Performed for Characterization

Test Performed	Test Description	Test Output	Test Step	Results
Bend Stiffness	2-point cantilever deflection	Driveshaft flexibility and how well it can track through tortuosity	5.1	6.1
Column Strength	Axial compression until buckle	Driveshaft push-ability	5.2	6.2
Kink Resistance	Axial compression until kink	Driveshaft ability to resist kinks during handling and tracking	5.2.2	6.3
Torsional Rigidity	Torque straight segment until peak torque or failure	Driveshaft ability to transfer torque	5.4	6.4
Tensile Elastic Response (Load vs. Elongation)	Axial tension until yield and failure	Driveshaft spring response	5.5	6.5

Bend fatigue test	Spin driveshaft on high speed in tight bend without traversing and measure time to failure	Driveshaft fatigue and wear performance in severe bend	5.6	6.6
Life Test	Spin driveshaft on high speed and traverse through carbon block to stress and wear the driveshaft	Driveshaft resistance to carbon abrasion and driveshaft life span during high speed rotation	5.7	6.7

5.1 Bend Stiffness Testing

5.1.1 The following steps were performed with an Instron tensile frame.

5.1.2 Set up the bend test fixture as shown in Figure 5.



Figure 5 Image of the bend test setup

5.1.3 Place the driveshaft specimen into the magnetic V-block with roughly half the driveshaft inside the V-block and half hanging off the end. See Figure 6 below.



Figure 6 Driveshaft specimen placed into V-block

- 5.1.4 Place a steel mandrel with OD \geq .050" that is magnetically attracted to the V-block on top of the driveshaft specimen to keep it rigidly attached to the V-block. The end of the pin gage/mandrel should line up with the edge of the V-block. See Figure 7 below.



Figure 7 Pin gage or mandrel held down by magnetic V-block and holding driveshaft specimen in place

- 5.1.5 Jog the crosshead of the tensile frame down until the center beam almost makes contact with the driveshaft. A gap of about 1 mm between the center beam and driveshaft is preferred. See Figure 8 below.
- 5.1.6 On the tensile frame, set this location as the gage length (this should set the displacement to zero) and balance the load cell to zero.
- 5.1.7 Slide the V-block left or right until the distance from the edge of the V-block

to the center beam (dimension x) is at the required setting. See Figure 8 below.

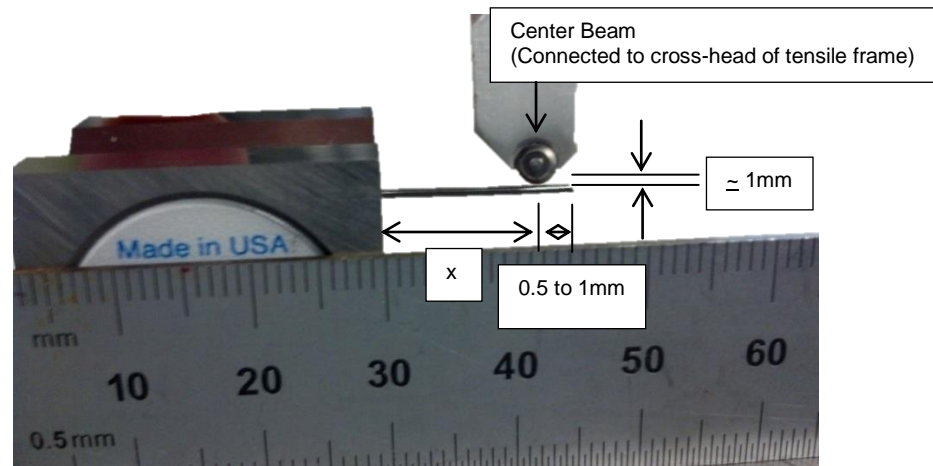


Figure 8 Diagram depicting gap between center beam and driveshaft and distance between edge of V-block and center beam.

- 5.1.8 Lift the mandrel away from the driveshaft and slide the driveshaft left or right in the V-block until the driveshaft hangs past the center beam by 0.5 to 1 mm. See Figure 8 above. Place the mandrel back onto the driveshaft and lined up against the V-block edge as shown above in Figure 7.
- 5.1.9 Set the tensile frame to compression mode so the center beam will deflect the driveshaft downward.
- 5.1.10 Set the crosshead speed to 0.5 in/min.
- 5.1.11 Set the test to stop at a total displacement of 0.15 in.
- 5.1.12 At a minimum, run the test at dimension x values of 10mm and 5mm.
- 5.1.13 Export the load versus displacement data to allow data analysis.

5.2 Column Strength Testing

- 5.2.1 The following steps were performed with an Instron tensile frame.
- 5.2.2 Ensure the 100N load cell is connected to the crosshead of the tensile

frame, as well as warmed up and calibrated.

5.2.3 Ensure the top and bottom pneumatic grips are connected to the tensile frame.

5.2.4 In the bottom grip, place a small plastic block that has a shallow hole to capture the end of the driveshaft. An example of a block that has been used for this test is shown below in Figure 9.

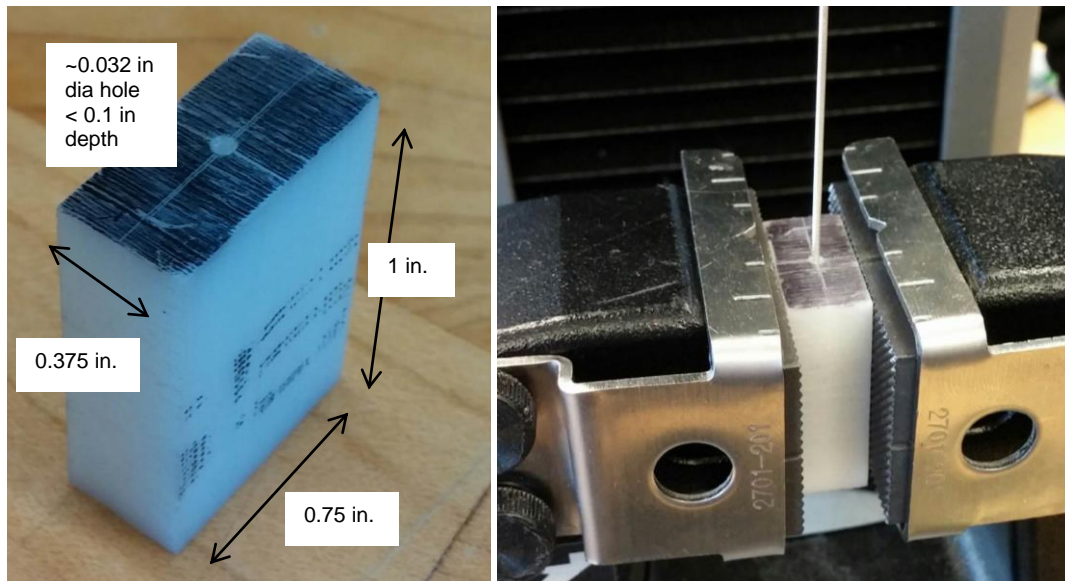


Figure 9 Left – An example of a block used to capture the bottom of the driveshaft. Right – The block is gripped in the pneumatic grips and holding the driveshaft.

5.2.5 Carefully place approximately 1.5 inches of driveshaft sample into the block from Figure 4.

5.2.6 Zero the load.

5.2.7 Set the grips to a gage length of 1 inch and zero the displacement.

5.2.8 Ensure the driveshaft is aligned approximately on axis with the tensile frame test direction.

5.2.9 Grip the top end of the driveshaft.

5.2.10 Set the tensile frame to compression mode so the test will compress the driveshaft downward.

5.2.11 Set the crosshead speed to 0.5 in/min.

5.2.12 Set the test to stop at a total displacement of 0.6 in, or a compressive strain of 60%.

5.2.13 Export the load versus displacement data to allow data analysis.

5.3 Kink Resistance

5.3.1 The data from section 5.2 was used to also calculate kink resistance.

5.4 Torsional Rigidity

5.4.1 The following steps were performed on the torsion test equipment.

5.4.2 Set up the torsion test equipment with the pin vise grips. See the equipment setup below in Figure 10.

5.4.3 Place a short mandrel in one end of the driveshaft and then place into the first pin vise grip and tighten so that the mandrel is completely inside the grip.

5.4.4 Place a short mandrel in the opposite end of the driveshaft. Move the second pin vise grip onto the driveshaft so the test length is 1 inch.

5.4.5 Ensure the mandrel is completely inside the grip and tighten the second pin vise grip.

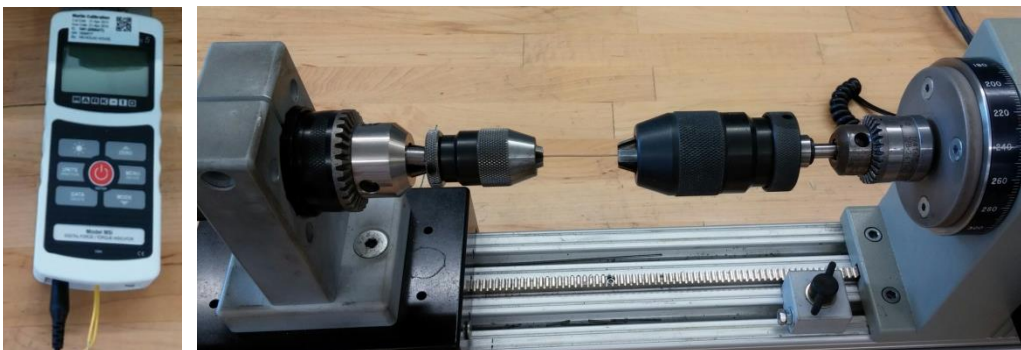


Figure 10 Left – Torque cell readout. Right – Torque test setup with pin vise grips. The vise grip on the left is connected to the torque cell and readout.

5.4.6 Torque the driveshaft until failure or until the maximum torque has been reached.

5.4.7 Each driveshaft design is to be tested in both clockwise and counter-clockwise directions.

5.4.8 Export the torque versus rotation data to allow data analysis.

5.5 Tensile Elastic Response (Load vs. Elongation)

5.5.1 The following steps were performed with an Instron tensile frame.

5.5.2 Set the grips to a gage length of 1 inch and zero the displacement.

5.5.3 Grip approximately 2 inch driveshaft sample in the top grip and ensure the driveshaft is aligned approximately on axis with the tensile frame test direction.



Figure 11 Driveshaft gripped in pneumatic grips.

5.5.4 Zero the load.

5.5.5 Grip the bottom end of the driveshaft.

5.5.6 Set the tensile frame to tension mode so the test will pull the driveshaft upward.

5.5.7 Set the crosshead speed to 0.5 in/min.

5.5.8 Set the test to stop at a total displacement of 2 inches.

5.5.9 Export the load versus displacement data to allow data analysis.

5.6 Bend Fatigue test

5.6.1 An orbital atherectomy device handle was assembled with a polymer driveshaft.

5.6.2 A tight bend model was created to challenge the driveshaft designs with both fatigue from spinning around the bend and abrasion from spinning over a guide wire. The apex of the bend goes down to a bend radius of 0.5 inches (12.7mm). When tracked through the model, the guide wire and driveshaft took a bend radius of approximately 0.87 inches (22mm). See Figure 12 below.

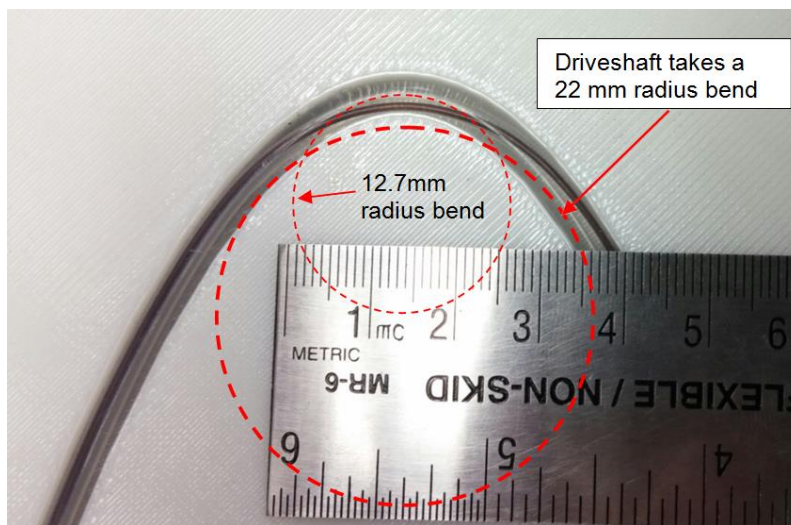


Figure 12 Driveshaft and guide wire tracked through the tight iliac model.

5.6.3 The device was spun using only water and no lubrication.

5.6.4 The polymer driveshaft was glued into the drivetrain of the handle using cyanoacrylate (Loctite).

5.6.5 The control knob was locked near the middle of the handle and the device was spun at 140krpm until failure.

5.6.6 This test only assessed the driveshaft performance while spinning around the bend. No crowns were used.

5.6.7 The time to failure was recorded.

5.7 Life Test

5.7.1 An orbital atherectomy device handle was assembled with a polymer driveshaft

5.7.2 The driveshaft was spun at 140krpm and passed through a simulation calcified lesion comprised of carbon graphite.

5.7.3 The device was spun for a total of 9 minutes, which is the required functional life span of an orbital atherectomy device.

6.0 RESULTS

6.1 Bend Stiffness

A minimum of two (2) driveshaft specimens were tested for each driveshaft design. The load versus deflection curve for each driveshaft was analyzed to calculate the slope of the elastic linear region. This slope of load versus deflection is the elastic bend stiffness. Figure 13 below shows a graph for the 5mm beam length test up to the yield point. Not all tested driveshaft designs are shown in Figure 13; however, they were all analyzed and compared below in Table 5.

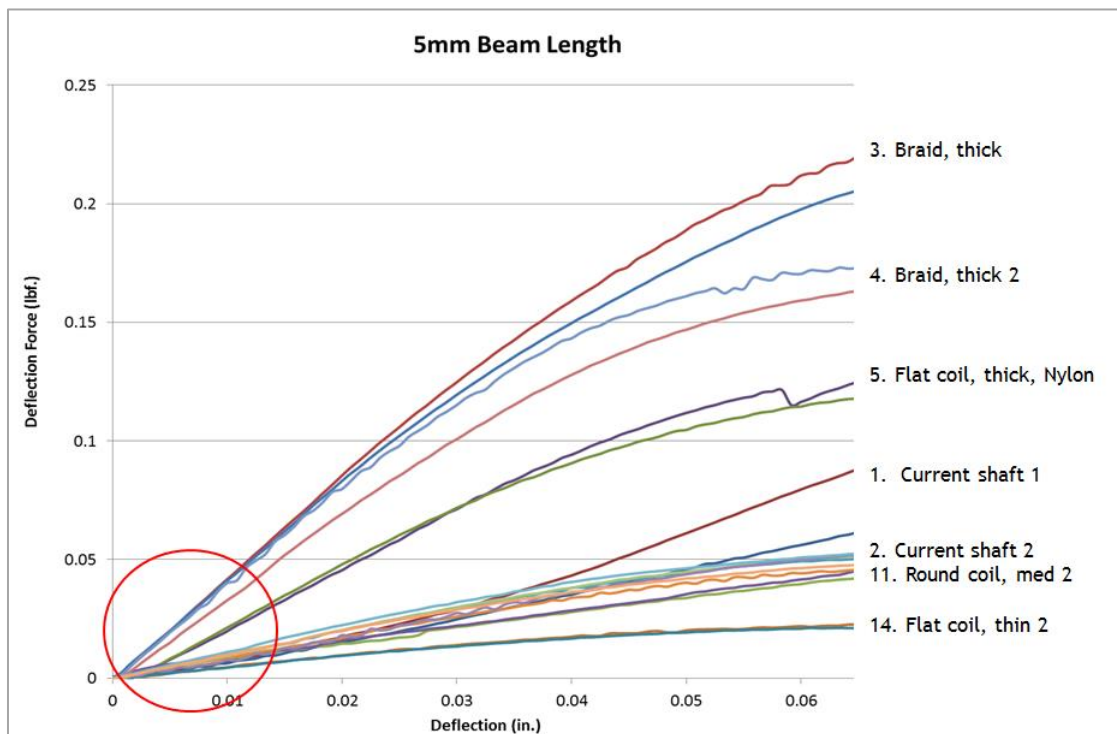


Figure 13 Load vs. Deflection curve for 5mm beam length stiffness test

Table 5 Calculated bend stiffness values for the tested driveshafts, sorted in descending order. The currently used driveshafts are shaded.

Driveshaft	5mm Beam (lbf/in)	10mm Beam (lbf/in)
3. Braid, thick	4.16	0.69
4. Braid, thick 2	3.66	0.61
5. Flat coil, thick, Nylon	2.40	0.38
10. Round coil, thick, Nylon	2.30	0.38
9. Round coil, med	1.93	0.37
17. Braid, med	1.92	0.44
6. Braid, thin	1.83	0.36
8. Round coil, thick	1.79	0.35
7. Flat coil, thin	1.01	0.19
11. Round coil, med 2	0.94	0.16
12. Flat coil, thin, Nylon	0.91	0.16
1. Current Shaft 1	0.77	0.14
2. Current Shaft 2	0.70	0.13
13. Round coil, thin	0.65	0.12
14. Flat coil, thin 2	0.47	0.10
16. Flat coil, thin 4	0.45	0.07
15. Flat coil, thin 3	0.31	0.06

6.2 Column Strength

A minimum of two (2) driveshaft specimens were tested for each driveshaft design. The compression load versus axial displacement curve for each driveshaft was analyzed to determine the buckle force. Figure 14 below shows the compression load vs. displacement graph for three of the tested driveshaft designs. All tested driveshafts were analyzed and compared below in Table 6.

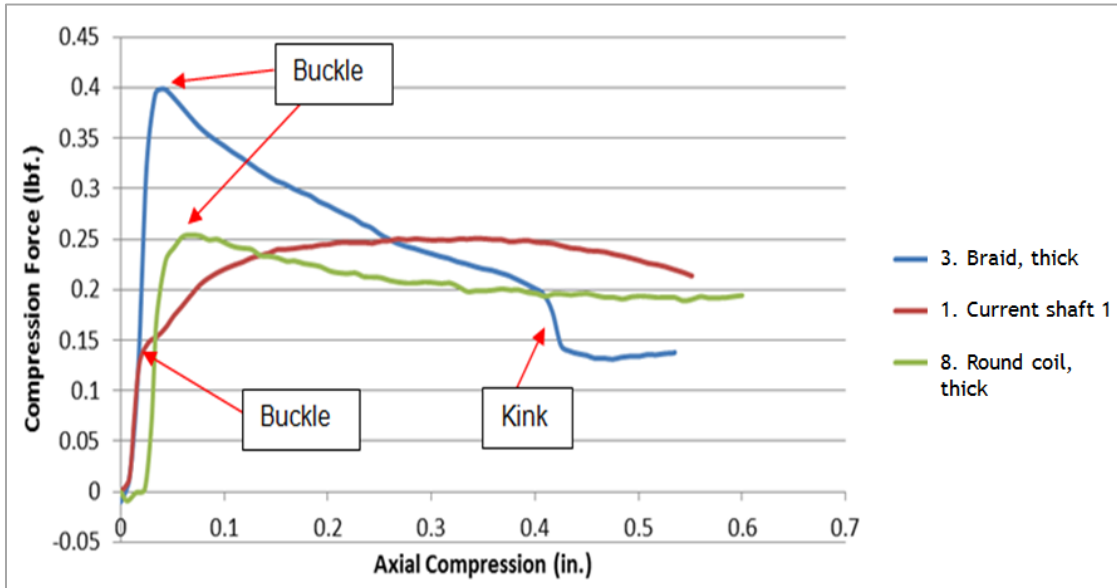


Figure 14 Compression load vs. displacement curve for three of the driveshaft designs.

Table 6 Buckle force and percent compression to kink for the tested driveshafts. The currently used driveshafts are shaded.

Driveshaft	Destructive Column Buckle Force (lbf.) (1 in. gage)	Destructive Column Buckle Compression to Kink (%) (1 in. gage)
3. Braid, thick	0.4	38%
4. Braid, thick 2	0.37	30%
8. Round coil, thick	0.31	no kink at 60%
5. Flat coil, thick, Nylon	0.29	12%
10. Round coil, thick, Nylon	0.26	slight kink at 60%
17. Braid, med	0.26	16%
9. Round coil, med	0.21	no kink at 60%
6. Braid, thin	0.18	16%
1. Current Shaft 1	0.15	no kink at 60%
12. Flat coil, thin, Nylon	0.11	12%
11. Round coil, med 2	0.10	no kink at 60%

Driveshaft	Destructive Column Buckle Force (lbf.) (1 in. gage)	Destructive Column Buckle Compression to Kink (%) (1 in. gage)
2. Current Shaft 2	0.08	no kink at 60%
7. Flat coil, thin	0.08	24%
13. Round coil, thin	0.06	40%
16. Flat coil, thin 4	0.05	53%
14. Flat coil, thin 2	0.05	12%
15. Flat coil, thin 3	0.03	40%

6.3 Kink Resistance

See Table 6 above for the column buckle force and kink testing. When compressed axially to 60% strain, there were 5 driveshaft designs that did not exhibit a kink, 2 of which were the current driveshaft designs.

6.4 Torsional Rigidity

A minimum of two (2) driveshaft specimens were tested for each driveshaft design. The torque versus rotation curve for each driveshaft was analyzed to calculate the slope of the elastic linear region. This slope of torque vs. rotation is the elastic torsion response. Figure 15 below shows a graph of torque vs rotation until failure for one driveshaft design. The calculated elastic torque response and maximum torque values are listed below in Table 7.

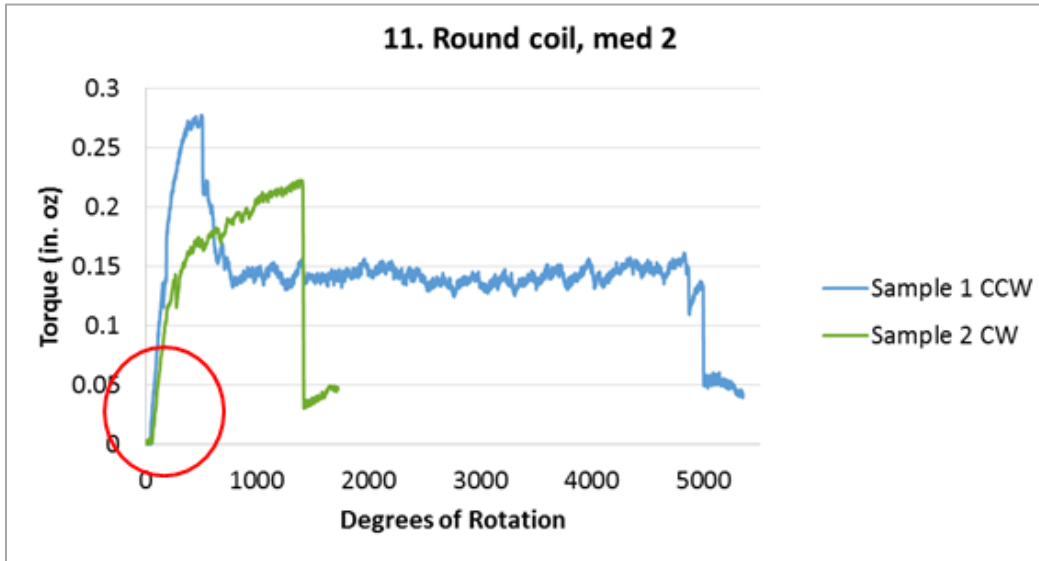


Figure 15 Torque vs. Rotation curve for one of the driveshaft designs

Table 7 Calculated elastic torque response and maximum torque values for the tested driveshaft designs. The currently used driveshafts are shaded.

Driveshaft	Clockwise Torsional Rigidity CW (Torque / Revolution)	Clockwise Peak Torque (in oz)	Counter- Clockwise Torsional Rigidity CCW (Torque / Revolution)	Counter- Clockwise Peak Torque (in oz)
3. Braid, thick	1.76	0.71	1.82	0.94
4. Braid, thick 2	1.63	0.53	1.66	0.80
17. Braid, med	not tested**	not tested**	1.31	0.65
8. Round coil, thick	0.85	0.89	0.76	0.63
10. Round coil, thick, Nylon	0.77	0.35	0.63	0.57
5. Flat coil, thick, Nylon	0.61	0.18	0.63	0.45
9. Round coil, med	0.49	0.38	0.59	0.48
1. Current Shaft 1	0.44	0.60	0.30	0.76
11. Round coil, med 2	0.28	0.22	0.48	0.29
12. Flat coil, thin, Nylon	not tested**	not tested**	0.43	0.18
7. Flat coil, thin	0.20	0.14	0.42	0.21
16. Flat coil, thin 4	0.20	0.04	0.22	0.15

Driveshaft	Clockwise Torsional Rigidity CW (Torque / Revolution)	Clockwise Peak Torque (in oz)	Counter-Clockwise Torsional Rigidity CCW (Torque / Revolution)	Counter-Clockwise Peak Torque (in oz)
13. Round coil, thin	0.12	0.06	0.20	0.22
14. Flat coil, thin 2	0.11	0.04	0.19	0.12
2. Current Shaft 2	0.10	0.54	not tested**	not tested**
15. Flat coil, thin 3	0.04	0.06	0.10	0.10

* A right-hand wound driveshaft that was tested with the clockwise setting resulted in rotating spin-to-close. All tested coil driveshafts, except for Current shaft 1, were left hand wound.

** Driveshaft had grip issues and testing was not completed

6.5 Tensile Elastic Response (Load vs. Elongation)

A minimum of two (2) driveshaft specimens were tested for each driveshaft design. The tensile force versus elongation curve for each driveshaft was analyzed to calculate the slope of the elastic linear region. This slope of force vs. elongation is the tensile elastic response. Figure 16 below shows a graph of force vs elongation until partial failure for three of the tested driveshaft designs. The calculated tensile elastic response and maximum force values for all tested driveshafts are listed below in Table 8.

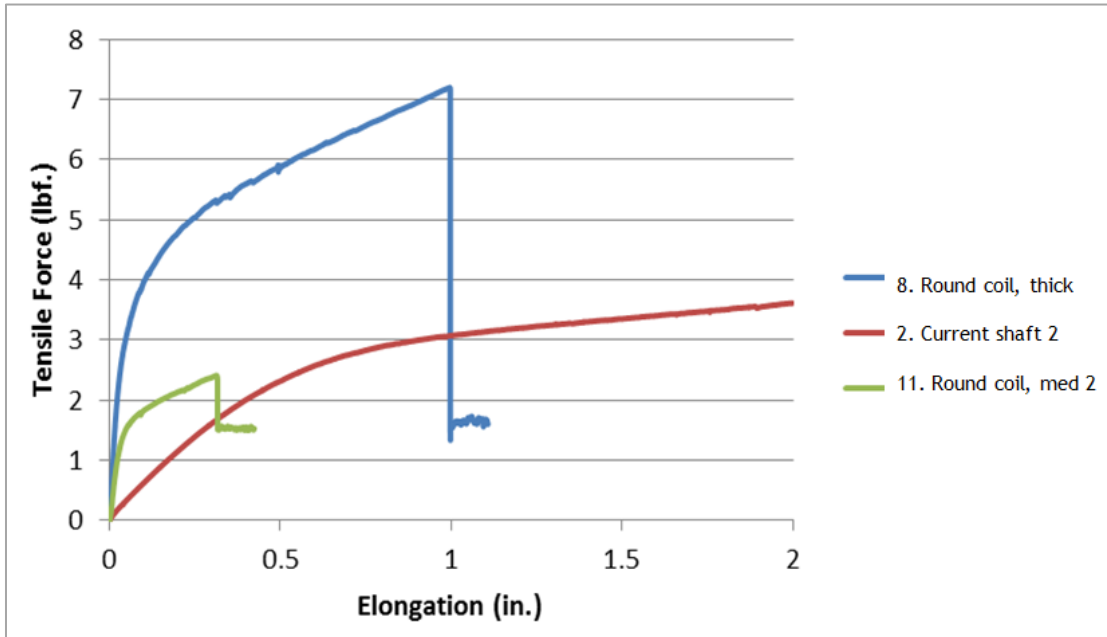


Figure 16 Load vs. Elongation curve for three driveshaft designs

Table 8 Calculated slope from the elastic region, maximum load reached, and elongation to initial failure. The currently used driveshafts are shaded.

Driveshaft	Average Elastic Slope (lbf/in)	Maximum Load (lbf)	Elongation to initial failure (in.)
3. Braid, thick	219.46	8.62	14.0%
4. Braid, thick 2	185.94	9.29	35.9%
17. Braid, med	132.69	6.91	25.1%
8. Round coil, thick	114.72	7.24	99.7%
9. Round coil, med	81.49	3.37	40.9%
10. Round coil, thick, Nylon	71.59	3.09	45.9%
7. Flat coil, thin	62.77	3.62	93.4%
5. Flat coil, thick, Nylon	58.70	2.28	>200%
11. Round coil, med 2	48.89	2.55	31.6%
13. Round coil, thin	38.49	2.02	145.6%
16. Flat coil, thin 4	35.45	2.89	76.8%
12. Flat coil, thin, Nylon	30.20	1.12	174.8%
15. Flat coil, thin 3	22.16	0.96	33.3%
14. Flat coil, thin 2	21.79	1.25	41.4%

Driveshaft	Average Elastic Slope (lbf/in)	Maximum Load (lbf)	Elongation to initial failure (in.)
1. Current Shaft 1	18.89	22.77	>200%
2. Current Shaft 2	6.58	3.61	>200%

All test results up to this point were analyzed and compared. Table 8 below compares all tested driveshafts and ranks from best to worst for each test performed.

Table 9 Ranking of driveshaft performance for each test. The current driveshafts (shaded) were used as the standard performance to be achieved.

+ 1 = Similar or better, 0 = Acceptable difference, -1 = Not close

Driveshaft	Bend Stiffness	Buckle Force	Kink Resist **2X Multiply	Torsion Rigidity	Peak Torque **2X Multiply	Elastic Tensile	Peak Tensile	Elong. to Fail	Score
1. Current Shaft 1									
2. Current Shaft 2									
8. Round coil, thick	0	0	+1	0	+1	+1	0	0	5
11. Round coil, med 2	0	+1	+1	+1	0	+1	-1	-1	3
9. Round coil, med	0	0	+1	0	0	+1	0	-1	2
13. Round coil, thin	+1	0	0	+1	-1	+1	-1	0	0
10. Round coil, thick, Nylon	0	0	0	0	0	+1	0	-1	0
17. Braid, med	0	0	-1	0	+1	+1	0	-1	0
3. Braid, thick	-1	-1	0	0	+1	+1	0	-1	0
7. Flat coil, thin	0	+1	-1	+1	-1	+1	0	0	-1
4. Braid, thick 2	-1	0	-1	0	+1	+1	0	-1	-1
16. Flat coil, thin 4	0	0	0	+1	-1	+1	-1	0	-1
12. Flat coil, thin, Nylon	0	+1	-1	+1	-1	+1	-1	0	-2
5. Flat coil, thick, Nylon	0	0	-1	0	-1	+1	-1	+1	-3
14. Flat coil, thin 2	0	0	-1	+1	-1	+1	-1	-1	-4
15. Flat coil, thin 3	-1	-1	0	-1	-1	+1	-1	-1	-6
6. Braid, thin	0	+1	-1	*	*	*	*	*	*

*Not tested – driveshaft was used for a different project.

**A 2X multiplier was applied to these scores due to their impact on functional use of the driveshaft.

6.6 Bend fatigue test

The top 3 driveshaft designs from Table 9 above were selected for testing in the tight bend model. Table 10 below lists the results of the bend fatigue testing.

Table 10 Results of the bend fatigue bend testing.

Driveshaft	Time to Failure 140krpm (m:ss)
8. Round coil, thick	4:30 (n=2)
11. Round coil, med 2	7:30 (n=1)
9. Round coil, med	4:30 (n=2)

Cross sections were collected on failed samples for driveshaft designs 8. Round coil, thick and 9. Round coil, med. See Figure 17 and Figure 18 below, respectively.

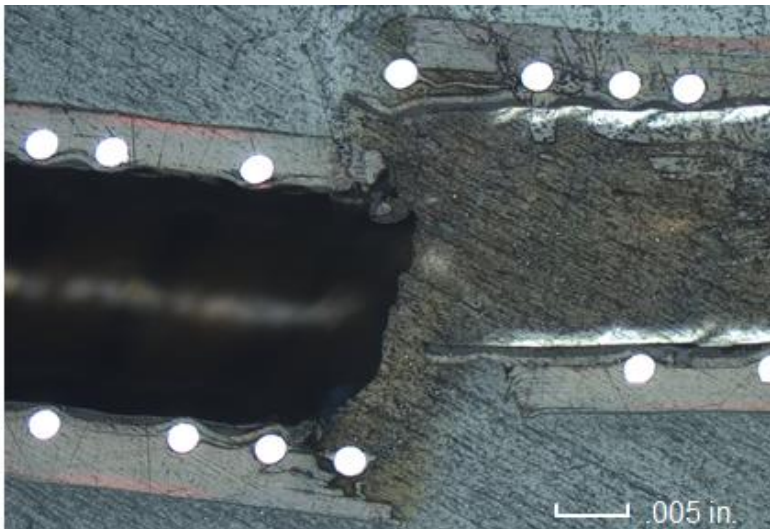


Figure 17 Cross section of failed 8. Round coil, thick driveshaft

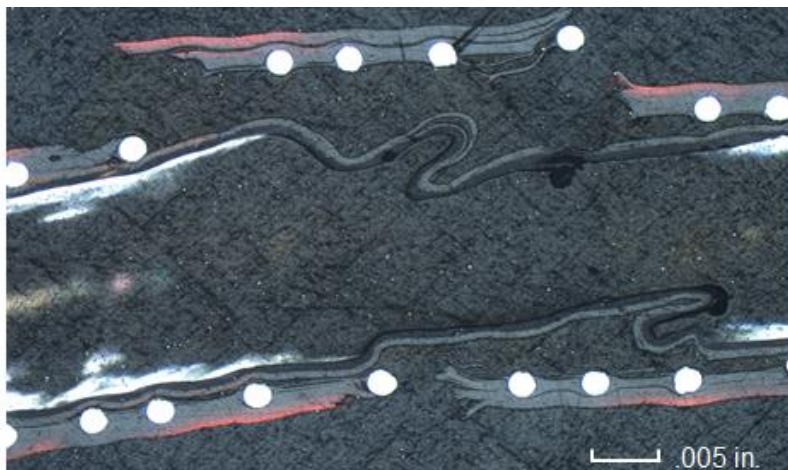


Figure 18 Cross section of failed 9. Round coil, med driveshaft

Analysis of the 8. Round coil, thick and 9. Round coil, med failure cross sections could not completely determine if failure was due to the coil pushing through the outer layer or delamination between the inner and outer polyimide layers because of a wavy inner layer. See Figure 19 below for a close view of the wavy inner layer on an untested 8. Round coil, thick driveshaft.

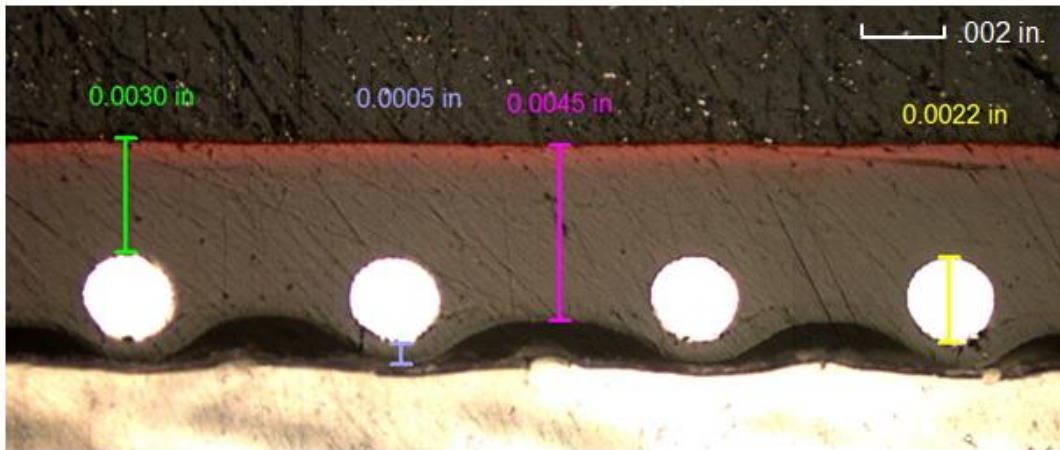


Figure 19 Cross section of an untested 8. Round coil, thick driveshaft. Note the wavy inner polyimide layer.

6.7 Life Test

A marker band was swaged (approximately .028" OD and .0015" thickness post-swaging) onto the end of an 8. Round coil, thick driveshaft. This marker band was used to laser weld a crown onto the driveshaft. The driveshaft was then put through life testing on high speed. After testing, the polymer driveshaft was analyzed and showed abrasion damage from the carbon during testing. See Figure 20 below.



Figure 20 Observed abrasion on the polyimide outer layer after life testing

Another 8. Round coil, thick driveshaft with similar marker band and crown was put through high speed stall testing. The device was spun at 140krpm and stalled 4 times and no damage was observed. The driveshaft still functioned with no issues. The stall transmitted torque values were comparable to stall values on current driveshafts.

7.0 CONCLUSIONS

This investigation has shown that a coiled metal wire with inner and outer polymer coating is a feasible driveshaft design and can meet the driveshaft design requirements.

Sample 8. Round coil, thick had the best overall average performance. This design had the best kink resistance due to the coiled round wire and the best torsional rigidity due to the polyimide material properties and thickness.

Although a feasible option has been identified, further investigation is recommended to improve certain aspects of the design. The polymer driveshaft should be tested against the current driveshafts to characterize and show reduced particulate ingress, reduced springing upon startup, and less influence on saline flow while spinning. Other aspects to investigate are thermoplastic materials or surface coatings for better abrasion resistance and thicker or different material inner layers to reduce waviness.

8.0 BIBLIOGRAPHY

1. Images from www.csi360.com
2. Equations from Roark's Formulas for Stress and Strain, W.C. Young and R.G. Budynas, 7th edition, 2002, pg. 189 and pg. 719
3. Data provided by supplier
4. Data from www.matweb.com